Distributed Multi-Period DCOPF via an Auxiliary Principle Problem Algorithm

Mohannad Alkhraijah, *Student Member*, *IEEE*, Maad Alowaifeer, *Student Member*, *IEEE*, Santiago Grijalva, *Senior Member*, *IEEE,* Daniel K. Molzahn, *Senior Member*, *IEEE*

***Abstract*—Distributed algorithms provide attractive features for solving Optimal Power Flow (OPF) problems in interconnected power systems compared to traditional centralized algorithms. Distributed algorithms help to maintain the control autonomy and data privacy of subsystems, which is particularly relevant in competitive markets and practical control system implementations. This paper analyzes a distributed optimization algorithm known as the "Auxiliary Principle Problem" to solve multiperiod distributed DCOPF problems with energy storage systems. The proposed approach enables multiple interconnected systems with their own sub-objectives to share their resources and to participate in an electricity market without implicitly sharing information about their local generators or internal network parameters. The paper also shows how the proposed approach can enable future microgrids to coordinate their operation, reduce the total operational cost, and avoid internal constraint violations caused by unscheduled flows (USF) while maintaining the subsystems' autonomy. We used an 11-bus test system consisting of two interconnected subsystems to evaluate the proposed approach and analyze the impact of USF.**

***Index Terms*— Aggregated microgrids, DCOPF, distributed optimization, unscheduled flow.**

I. Introduction

A. Motivation

OPTIMAL power flow (OPF) is one of the fundamental problems in power systems with a wide variety of applications in security assessment, market operations, and long-term planning. The OPF problem aims to find the optimal operating setpoints for generating units and other controls in a power system. Common objectives of the OPF problem include minimizing the generation cost, the total power losses, and the voltage deviations from nominal values [1]. Many solution algorithms and methodologies have been proposed since the OPF problem was introduced in 1962 [2]. The deployment of distributed energy resources (DERs) such as distributed generation, energy storage systems (ESS), and controllable loads pose significant challenges to the OPF problem in terms of scalability, information exchange, and system complexity [3-4].

Conventionally, the OPF problem is solved in a centralized manner, where the computation is done by a grid operator who has access to a detailed network model, receives information about the system state in real-time, runs the optimization, and sends back the optimal setpoints to the controllable resources. The recent emergence of microgrids as independent subsystems that operate their local DERs and interact with the larger power system increases the difficulty of solving the OPF problem [5-6]. The active behavior of the DERs can introduce power injection variability that challenges the grid operator's ability to accurately model the system and determine appropriate setpoints. The grid operator usually models the internal network of small independent subsystems with an equivalent circuit [7], making it difficult to ensure satisfaction of network constraints within these subsystems.

B. Unscheduled Flow

Growing quantities of independently operated subsystems could compromise system reliability due to unscheduled flows (USF), i.e., loop flows [8]. USF is defined as the mismatch between the actual and scheduled power flows. The actual power flow is governed by the network topology characterized by the lowest impedance path, while the scheduled flow is determined by market clearing. USF is a widely studied problem in both academia and industry, particularly with respect to the shared use of transmission infrastructure [8-11]. Problems resulting from USF have been also attributed to major blackouts and equipment damage [9-10].

USF is expected to occur more frequently in deregulated markets [11]. Researchers have recently proposed new concepts such as peer-to-peer (P2P) markets in order to enable microgrids to directly share their resources with other microgrids [12]. Interconnected microgrids with high DERs penetration capable of participating in P2P energy trading might compromise system reliability due to constraint violations from USF. Coordinating the microgrids using a centralized controller avoids problems associated with USF. However, this requires sharing the microgrids' internal network details and local generation costs with the centralized controller, which raises concerns regarding data privacy. These challenges motivate the use of distributed optimization algorithms.

C. Distributed Optimal Power Flow

Distributed optimization algorithms have the potential to address important challenges in future power systems. A survey of different applications of distributed algorithms in power systems including OPF is provided in [13]. In distributed approaches, the OPF problem is segmented into smaller independent subproblems. Each subproblem represents a subsystem, e.g., a microgrid, that can be controlled and operated by a local controller. Each local controller solves the subproblem and shares the results with other subsystems. An iterative process is then implemented between the subsystems to achieve the optimal solution without sharing the generation cost information.

Fully distributed OPF solution approaches have many potential advantages over centralized approaches including (a) providing scalable computation as long as the coupling between the subsystems is sparse [14], (b) allowing parallel computation as each subsystem will solve the associated subproblem independently, (c) limiting the amount of shared data, providing the possibility for increased privacy, (d) reducing the communication infrastructure requirements since each subsystem only needs to communicate with neighboring subsystems, (e) increasing robustness against a single point of failure, and (f) providing modularity and flexibility to cope with the frequent changes in the subsystems.

D. Literature Review

The advantages of the distributed optimization in solving the OPF motivate research into different distributed algorithms, e.g., Alternating Direction Method of Multipliers (ADMM) [14-15], Auxiliary Principle Problem (APP) [16-17], , and Analytical Target Cascading (ATC) [18]. Numerical comparisons among different distributed algorithms is provided in [19-20]. Notably, the distributed OPF methods in [13-20] do not consider time-variant models to solve multiperiod OPF. To model time-variant DERs such as Energy Storage Systems (ESS), an extension to the distributed OPF problem is necessary.

Zhu et al. [21] proposed a multiperiod OPF formulation considering a configuration of meshed microgrids connected radially to the main grid with a three-phase unbalanced network. Distributed algorithms have been applied with convex relaxation methods for multiperiod OPF problems. A multiperiod OPF formulation is proposed in [22] using the branch flow model for radial networks. The authors of [22] also consider a three-phase unbalanced network and use ADMM to solve the ACOPF problem. In [23], an SDP relaxation is iteratively solved using ADMM. The global optimality guarantees for convex relaxation methods are limited to radial networks that satisfy additional technical conditions [24-25]. The models proposed to solve the multiperiod timestep are either radially or semi-radially connected microgrids, i.e., the subsystems themselves are not directly interconnected.

In [26], a multiperiod DCOPF problem considering carbon emission trading is solved using an ADMM-based distributed algorithm for interconnected subsystems. An ADMM-based distributed algorithm is proposed in [27] to solve the ACOPF problem considering demand response and discrete variables for real-time pricing applications. The convergence of different OPF formulations is compared with and without the discrete variables. The study shows that a quadratic ACOPF using convex relaxation formulations as proposed in [5] is the fastest in many cases; however, the distributed algorithms are only guaranteed to converge for a convex problem, which is not the case for ACOPF problems. The same algorithm also shows a stable convergence for the DCOPF problem.

The interest in using distributed algorithms to solve the OPF problem has been increasing in recent years, motivated by the promising features desired for future power systems. Nonetheless, there are potential advantages and unexpected disadvantages that have not been explored when considering practical implementations of distributed algorithms.

E. Contribution

This paper explores the application of the APP algorithm to multiperiod DCOPF problems. The APP algorithm enables a fully distributed approach that permits co-optimizing multiple microgrids/subsystems while respecting their internal constraints. Using a small test system as a proof of concept, we show the APP algorithm's ability to coordinate an electricity market in a distributed fashion while avoiding internal constraint violations that might arise due to USF.

F. Paper Organization

This paper is organized as follows. Section II formulates the centralized multiperiod DCOPF problem. Section III introduces the distributed multiperiod DCOPF problem based on the APP formulation. Section IV demonstrates the USF impacts and discusses the distributed OPF implementation. Finally, Section V concludes the paper and presents future work.

II. Centralized DC Optimal Power Flow

The OPF problem considered in this paper minimizes the total generation cost for multiple interconnected subsystems that are connected to the main grid at the point of common coupling (PCC). We use a multi-period formulation appropriate for ESS. The optimization variables are the power flow from/to the grid, the active power generation, and the voltage angles. The solution must satisfy engineering constraints including active power generation, ramp rate, and line flow limits. The DC approximation of the power flow used in this paper is shown in (1) [28].

$$\min_{(p_i,\theta_i)} \sum_{t\in T}\sum_{a\in\mathcal{G}} f_a(p_{a,t}) - \pi_t\, p_{PCC,t} \tag{1.1}$$

subject to:

$$p_{i,t} - p_{i,t}^{SC} + p_{i,t}^{SD} - P_{i,t}^{d} = \sum_{(i,j)\in\mathcal{L}} B_{ij}(\theta_{i,t}-\theta_{j,t}) \tag{1.2}$$

$$E_{b,t} - E_{b,t-1} - \eta\, p_{b,t}^{SC} + \frac{1}{\eta}\, p_{b,t}^{SD} = 0 \tag{1.3}$$

$$P_a^{min} \le p_{a,t} \le P_a^{max} \tag{1.4}$$

$$-P_{ij}^{max} \le B_{ij}(\theta_{i,t}-\theta_{j,t}) \le P_{ij}^{max} \tag{1.5}$$

$$-R_a^{down} \le p_{a,t-1} - p_{a,t} \le R_a^{up} \tag{1.6}$$

$$\theta_t^{ref} = 0 \tag{1.7}$$

$$\forall\, i\in\mathcal{N},\ a\in\mathcal{G},\ b\in\mathcal{B},\ (i,j)\in\mathcal{L},\ t\in T$$

where π is the price of active power from the main grid at the PCC. The decision variables are the generator active power output p and the voltage angles θ. The sets $\mathcal{N}$, $\mathcal{G}$, $\mathcal{L}$, and $\mathcal{B}$, respectively, correspond to the system buses, generators, lines, and ESS. P^d is the power demand. p^{SC} and p^{SD} are the ESS's charging and discharging power, while E is the energy state and η is the efficiency of the ESS. p^{max} and p^{min} are the upper and lower bounds on the generators' power outputs. P_{ij} is the line flow from bus i to bus j. P_{ij}^{max} is the upper bounds on the power flow from bus i to bus j, while B_{ij} is the (i,j) entry of the susceptance matrix as defined in [28]. R^{up} and R^{down} are the generators' ramp up and ramp down rates. (1.2) – (1.8) are the equality and inequality constraints of the DCOPF. (1.2) is the DC approximation of the power flow, and (1.3) is the energy balance of ESS. (1.4) – (1.6) are the engineering constraints, while (1.7) sets the reference angle. In this formulation, the PCC is represented as a bus with a connected generator that can produce or absorb active power to model importing and exporting power from the main grid.

III. Distributed DC Optimal Power Flow

We use APP, the distributed optimization algorithm proposed in [16], with an extension to incorporate a linear ESS dynamic model. The APP algorithm requires decomposing the problem into smaller subproblems with shared variables and coupling constraints. Each subproblem is associated with a subsystem, and the tie-lines between subsystems model the coupling constraints. In the DCOPF case, the subsystems share the voltage angles of the tie-line terminals with the neighboring subsystems. We introduce dummy variables θ' to replicate the shared variables θ. Fig. 1 illustrates the shared variables before (a) and after (b) introducing the dummy variables between two subsystems. Then, we use consistency constraints to bind the dummy variables θ' with the respective shared variables. We then relax the constancy constraints using the augmented Lagrangian to eliminate the coupling between the subsystems' internal constraints assuming the dummy variables are constants.

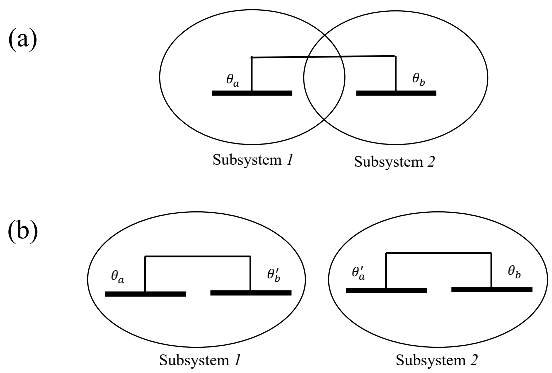

Fig 1. (a) An example of two subsystems connected through tie-line between bus *a* and *b*. (b) Dummy variables that duplicate the shared variables for this example.

Let $\mathcal{N}_m$ and $\mathcal{L}_m$ define the sets of buses and lines at subsystem $m \in \mathcal{M}$, where $\mathcal{M}$ denotes the set of subsystems. Let $\mathcal{G}_m$ and $\mathcal{B}_m$ denote the sets of generators and ESSs at subsystem m. Let $\mathcal{N}_m^s$ define the set of all shared variables at subsystem m. The tie-lines between any local shared variable and a neighboring shared variable are denoted by the set $\mathcal{L}_m^s$. Using the formulation of the APP proposed in [16], the optimal solution of problem (1) is found by solving a sequence of subproblems. At each iteration, all of the subproblems are solved at the same time by local controllers. The result of each subproblem is then shared with the neighboring subsystems. Afterword, each subsystem solves the local subproblem again using the newly shared information to evaluate the dummy variables. The process is repeated until the stopping criterion is met. The subproblem for subsystem m at iteration $k+1$ is shown in (2).

$$\min_{\left(p_{a,t}^{k+1},\theta_{i,t}^{k+1}\right)} c + \xi^p + \xi^c \tag{2.1}$$

$$c = \sum_{t\in T}\sum_{a\in\mathcal{G}_m} f_a\left(p_{a,t}\right) - \pi_t\, p_{PCC,t} \tag{2.1.1}$$

$$\xi^p = \sum_{t\in T}\sum_{i\in\mathcal{N}_m^s} \frac{\beta}{2}\left\|\theta_{i,t}^{k+1} - \hat{\theta}_{i,t}^{k}\right\|^2 \tag{2.1.2}$$

$$\xi^c = \sum_{t\in T}\sum_{i\in\mathcal{N}_m^s}\left(\gamma\theta_{i,t}^{k+1}\left(\hat{\theta}_{i,t}^{k} - \hat{\theta}'^{k}_{i,t}\right) + \lambda_{i,t}^{k}\,\theta_{i,t}^{k+1}\right) \tag{2.1.3}$$

subject to:

$$p_{i,t}^{k+1} - p_{i,t}^{SC,k+1} + p_{i,t}^{SD,k+1} - P_{i,t}^{d,k+1} = \sum_{(i,j)\in\mathcal{L}_m^s} B_{ij}\left(\theta_{i,t}^{k+1} - \theta_{j,t}^{k+1}\right) \tag{2.2}$$

$$E_{b,t}^{k+1} - E_{b,t-1}^{k+1} - \eta\, p_{b,t}^{SC,k+1} + \frac{1}{\eta}\, p_{b,t}^{SD,k+1} = 0 \tag{2.3}$$

$$P_a^{min} \le p_{a,t}^{k+1} \le P_a^{max} \tag{2.4}$$

$$-P_{ij}^{max} \le B_{ij}\left(\theta_{i,t}^{k+1} - \theta_{j,t}^{k+1}\right) \le P_{ij}^{max} \tag{2.5}$$

$$-R_a^{down} \le p_{a,t-1}^{k+1} - p_{a,t}^{k+1} \le R_a^{up} \tag{2.6}$$

$$\theta_{m,t}^{ref} = 0 \tag{2.7}$$

$$\forall\, i\in\mathcal{N}_m,\ a\in\mathcal{G}_m,\ b\in\mathcal{B}_m,\ (i,j)\in\mathcal{L}_m,\ t\in T$$

where c is the operational cost, ξ^p is a penalty term for the deviation from the solution of the previous iteration, and ξ^c is another penalty term for mismatches of the relaxed consistency constraints. The notation $\|\,.\,\|$ indicates the L_2 norm. β and γ are parameters whose values are discussed in Section IV-B. The hat superscript in (2.1) indicates known variables. λ is the Lagrange multiplier of the consistency constraints. At each iteration, the Lagrange multipliers are updated as:

$$\lambda_i^{k+1} = \lambda_i^k + \alpha\left(\hat{\theta}_i^{k+1} - \hat{\theta}'^{k+1}_i\right) \tag{3}$$

where α is a parameter. The solution method is shown in Algorithm 1. We used bold letters to indicate vectors. The optimal solution is obtained by iteratively solving the subproblems (2), sharing the optimal solutions between the subsystems, and updating the Lagrange multipliers according to (3). Observe that the parameters appearing in (2.1.1), the cost function parameters, and (2.1.2), the parameter β, are fixed throughout the iterations, while (2.1.3) is not, as it contains the Lagrange multipliers updates λ. Conceptually, λ indicates how the subsystems value the power at the tie-line based on the shared information. As the iterations proceed and λ is updated, the value of importing/exporting power changes accordingly. The process continues until either consistency is achieved, i.e., the maximum mismatch is less than a predefined tolerance value ε, or the maximum number of iterations k^{max} is reached. Achieving consistency can be interpreted as the subsystems agreeing on the value of the Lagurange multiplier λ. The algorithm is proven to converge to the optimal solution of the original problem if all the subproblems are convex and differentiable, which is the case with the DCOPF problem [29-30].

Algorithm 1: DC-OPF Using APP

Initialize $\boldsymbol{\theta}, \boldsymbol{p}, \boldsymbol{\lambda}, \alpha, \beta, \gamma, k^{max}, \varepsilon$, and set $k = 1$
while $\left\|\boldsymbol{\theta}^{k+1} - \boldsymbol{\theta}'^{\,k+1}\right\|_\infty > \varepsilon$ and $k < k^{max}$ **do**
  Solve (2) $\forall\, m \in \mathcal{M}$ (in parallel)
  Share $\theta_i, \forall i \in \mathcal{N}_m^s, m \in \mathcal{M}$ with neighbors
  Update $\boldsymbol{\lambda}$ using (3)
  $k = k + 1$
end while

IV. Results and Discussion

A. Test Case and Simulation Setup

The system we study in this paper consists of two interconnected subsystems adapted from the test case "WB5" in [31] as shown in Fig.2. The ratings in Fig. 2 are in per unit with a base power of 100 MVA. The first digit of the bus names indicates the subsystem number, while the second digit is the bus number. We introduce an infinite bus representing the *PCC* that is connected to the buses *11* and *21* thorough lines *L1* and *L2*, and a tie-line *L3* connecting the two subsystem between the buses *13* and *22*. We place two local generators with 100 MW and 250 MW power capacity at bus *5* of both subsystems. The generation cost is \$30.90/MWh for P_{G15} and \$19.00/MWh for P_{G25}. Subsystem *2* has a 250 MW peak solar generator at bus *24*. Two ESSs with 50 MW/100 MWh and 100 MW/200 MWh are placed at bus *4* in each subsystem. The ESS's efficiency is 95%. The internal lines' flow limit is 200 MW, and the lines from the subsystems to the *PCC* have a 300 MW limit.

We use data obtained from [32] with random perturbations for the hourly demands. We also use price signal data obtained from [33] and one day of PV power output from NREL [34]. The data used in the implementation is shown in Fig. 3. We assume that the energy will be purchased and sold at the same price and the subsystems are price takers. The implementation uses MATLAB version 2020a and CPLEX solver version 12.10 with a personal computer with 2.8GHz Quad-Core Intel Core i7 and 16GB of RAM.

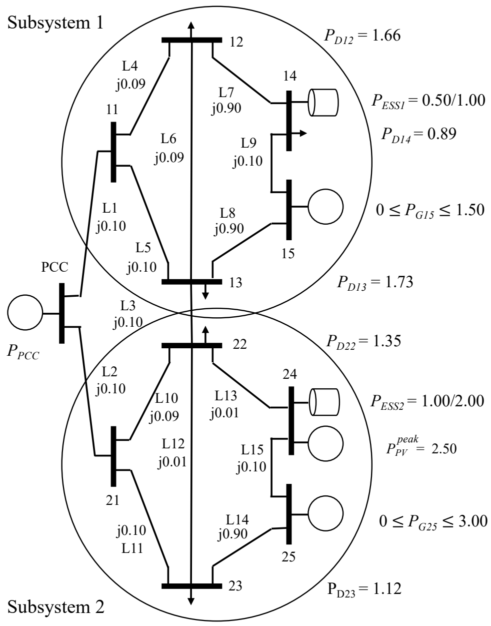

Fig 2. Modified five-bus system from [33] with impedances and peak powers in per unit with base power of 100 MVA.

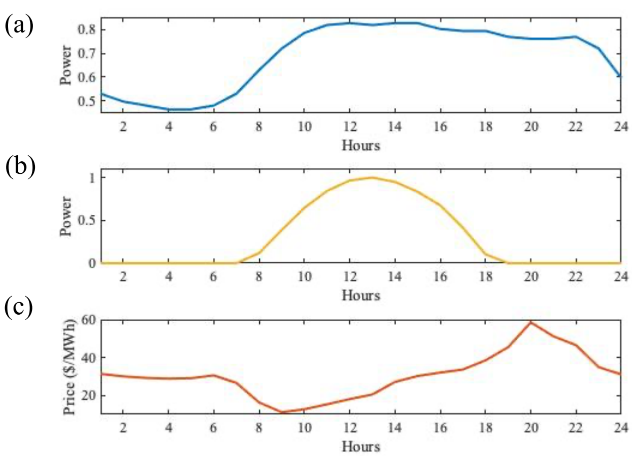

Fig 3. Case study datasets (a) normalized demand data, (b) normalized solar energy output power, and (c) the price signal.

B. Unscheduled Flow Evaluation

To demonstrate the USF, we first consider independent operation of the two subsystems. In this case, each subsystem will solve DCOPF independently. Using optimal control setpoints obtained from each subsystem, we used DC power flow to calculate the actual flow. Fig. 4 shows the maximum daily power flows on each transmission line. If the two systems operate according to this schedule, the flows on the tie-line *L3* and the internal line *L12* in subsystem *2* violate the line flow limits by 1.5% (3 MW) and 15% (30 MW), respectively, due to the USF as highlighted in red in Fig. 4. The actual value of the maximum USF at each line is shown in Fig. 5.

To avoid violating the line flow limits, we consider two scenarios: (a) removing the tie-line and (b) coordinating the optimization of both subsystems. While eliminating the tie-line will prevent USF, the subsystems will not be able to share their resources without going through the *PCC*. The proposed APP algorithm is well suited for the second scenario as it can coordinate the operation of the subsystems, accounting for the internal constraints without explicitly sharing their data.

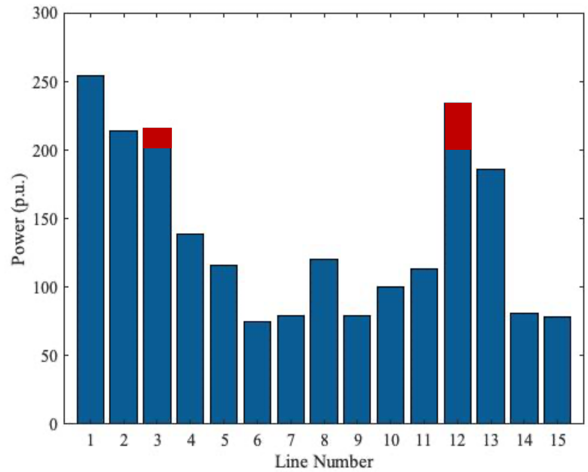

Fig. 4. Maximum daily line flow when optimized independently, with line limit violations highlighted in red.

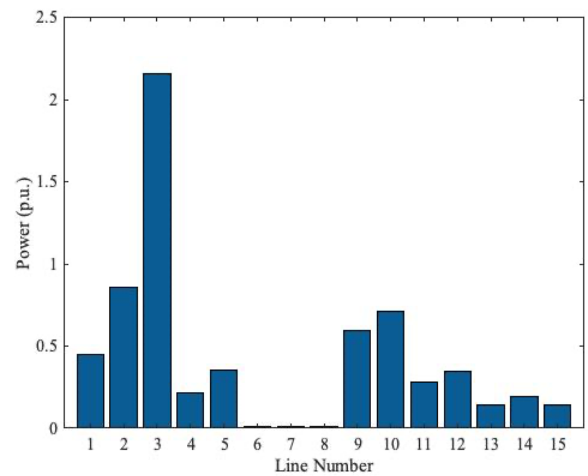

Fig. 5. Maximum daily USF when optimized independently.

C. Coordinated Results

Using the APP algorithm, we solved the DCOPF problem for the test system. We used flat start to initialize the algorithm and error tolerance equal to 10^{-4}. Fig. 6 shows the power profiles of each subsystem and Fig. 7 shows the export/import power. Between 08:00 and 13:00, the low energy prices result in both subsystems importing energy from the main grid. During the high-price periods from 15:00 to 20:00, both subsystems operate their local generation units at their maximum outputs to supply their local demands and export excess energy to the grid. Both subsystems use their ESSs to sell energy during the high-price periods from 06:00 to 14:00, and subsystem *1* imports energy from both the main grid and subsystem *2*.

Table I shows the operational costs of the two subsystems without coordination and with coordination using APP. The negative signs in Table I indicate the revenue from exporting energy to the grid. The price signal at the *PCC* is used to calculate the operational cost for both subsystems. For comparison purposes, we used the aggregated cost of the two subsystems to calculate the overall operating cost. The overall operation cost is reduced by \$3450 when we calculate the aggregated operation cost. In this case, both subsystems benefit from sharing their resources, as the operating cost of subsystem *1* decreases by \$3180, while the revenue of subsystem *2* increases by \$202.

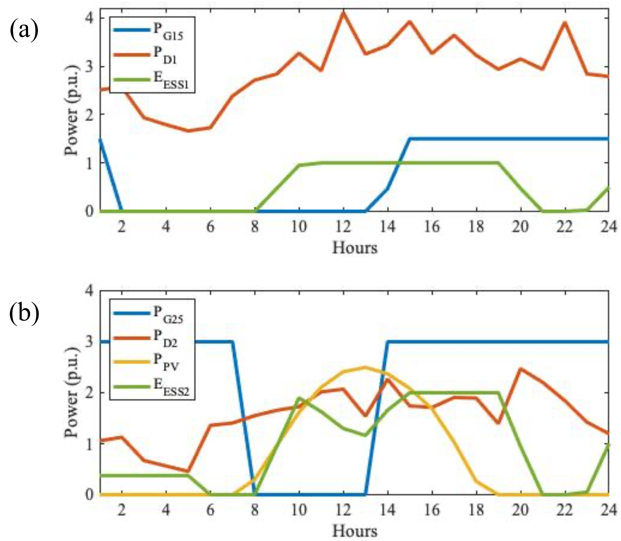

Fig. 6. Optimal schedule for (a) subsystem *1* and (b) subsystem *2*.

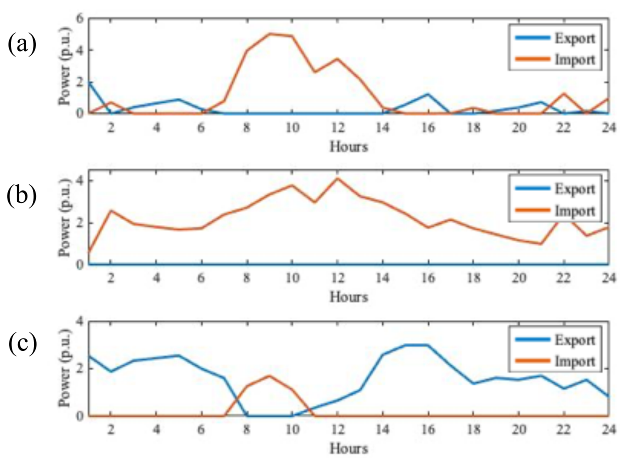

Fig. 7. Export and import for (a) the aggregation of the two subsystems, (b) subsystem *1*, and (c) subsystem *2*.

TABLE I
THE TOTAL OPERATION COST IN \$

Coordination	**Independent Optimization**	**Coordinated Optimization**
Subsystem *1*	198330	195150
Subsystem *2*	-16946	-17214
Aggregation	181380	177930

D. APP Tuning and Convergence

The rate of convergence for the APP algorithm depends on the values for the parameters α, β, and γ. Satisfying condition (4) is sufficient to guarantee convergence of the APP algorithm [16]. We used (5) to express all constants in terms of a single parameter in order to simplify the tuning analysis.

$$\alpha \leq 2\gamma \leq \beta \tag{4}$$

$$\alpha = \frac{1}{2}\beta = \gamma \tag{5}$$

The convergence of the APP algorithm with different values of α is shown in Fig. 8. The APP algorithm converges to a solution with an objective value gap within 0.001% of the centralized algorithm's solution. As the value of α increases, the convergence time and the number of iterations decreases as shown in Table II. However, increasing the value of α to 5×10^5 causes the convergence to be less consistent and slower. Furthermore, increasing the value of α above 5×10^5 causes the algorithm to diverge. The reverse is also true when the value of α is very small.

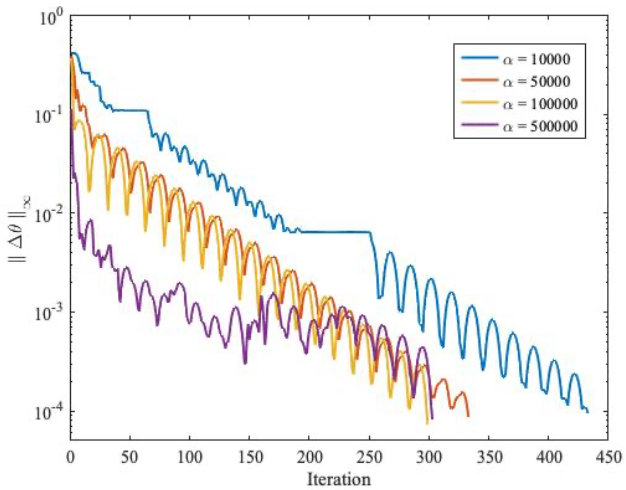

Fig. 8. Error convergence with different values of α.

TABLE II
PERFORMANCE EVALUATION WITH DIFFERENT VALUES OF α

α	1×10^4	5×10^4	1×10^5	5×10^5
No. Iteration	433	333	299	303
Avg. Iteration Time (s)	0.07	0.07	0.07	0.07
Total Time (s)	31.65	23.66	20.42	20.76

E. Discussion and Remarks

The APP algorithm converges to the optimal solution of the DCOPF problem. However, the APP algorithm has some limitations related to computation times and parameter tuning. The APP algorithm takes longer time to coverage compared to the centralized optimization, and the parameters tuning is system dependent, which implies the need for parameters tuning when considering a new system. Nonetheless, the APP algorithm has important features that can benefit future microgrids in deregulated markets. A deregulated scheme such as P2P markets could give rise to undesirable operation unless the underlying physics and their constraints are considerted. USF is expected to increase due to high penetrations of DERs that actively participate in deregulated markets. USF is especially problematic when there are interconnections between independently operated subsystems.

The implementation of the proposed algorithm could vary depending on the regulations and the market structure. The APP algorithm requires each subsystem to at least communicate the tie-lines' susceptance and terminal voltages. In our test case, Subsystem *2* extensively exports energy during periods of high solar power output, when the line limit violation was observed. The high solar energy output coincides with low-priced energy leading to line flow violations. Similar scenarios could occur for any system with many DERs and multiple independently operated interconnected subsystems.

V. Conclusion

Distributed algorithms provide many desirable features for future electricity markets. The high expected DER penetrations and the emergence of microgrids, i.e., independently operated subsystems, will require flexible optimization tools to cope with the system complexity. We use a small test case to demonstrate the potential impact of operating independent power systems, focusing on internal constraint violations due to USF. The APP algorithm allows independent subsystems to co-optimize their operation while satisfying their internal constraints without explicitly sharing information about generation cost or internal network data. Hence, the subsystems may pool their resources and increase the resultant system-wide profits from market participation.

The linearity of the DC approximation allows us to explore the capabilities of the distributed algorithms for market clearing with multiple microgrids in a multiperiod setting. In our future work, we plan to explore other power flow approximation and relaxation methods in order to extend our analyses to systems for which the DC power flow is inapplicable. Further, the communication system plays a major role in the performance of distributed algorithms, as the data will be shared continuously between the neighboring subsystems. We will investigate the implementation of distributed algorithms considering nonideal communication models.

References

[1] H. W. Dommel, W. F. Tinney, "Optimal power flow solutions," *IEEE Transactions on Power Apparatus and Systems*, vol. PAS-87, no. 10, pp. 1866-1876, Oct. 1968.

[2] J. Carpentier, "Contribution a l'Etude du Dispatching Economique," *Bull. Soc. Francaise des Electriciens*, vol. 3, pp. 431–447, Aug. 1962.

[3] "Quadrennial technology review: An assessment of energy technology and research opportunities: Chapter 2: Energy sectors and systems," US Department of Energy, Sept. 2015.

[4] J. Liu, M. Benosman, A. U. Raghunathan, "Consensus-based distributed optimal power flow algorithm," *IEEE Power & Energy Society Innovative Smart Grid Technologies Conference (ISGT)*, Washington, DC. Feb. 2015.

[5] M. Kraning, E. Chu, J. Lavaei, S. Boyd, "Dynamic network energy management via proximal message passing," *Foundation and Trends in Optimization*, vol. 1, no. 2, pp. 73–126, Jan. 2013.

[6] J. Guerrero, P. Loh, M. Chandorkar, and T. Lee, "Advanced control architectures for intelligent microgrids - Part I: Decentralized and hierarchical control," *IEEE Transaction on Industrial Electronics*, vol. 60, no. 4, pp. 1254–1262, April 2013.

[7] S. Deckmann, A. Pizzolante, A. Monticelli, B. Stott, and O. Alsac, "Studies on power system load flow equivalencing," *IEEE Transaction Power Apparatus and* Systems, vol. PAS-99, pp. 2301–2310, Nov. 1980.

[8] A. Q. Dozier, S. Suryanarayanan, J. P. Liberatore and M. C. Veghte, "Unscheduled flow in deregulated electricity markets: Bridging the gap between the western electric power industry and academia," *IEEE Green Technologies Conference*, Denver, CO, pp. 451-458, April 2013.

[9] J. A. Kavicky and S. M. Shahidehpour, "Parallel path aspects of transmission modeling," *IEEE Transactions on Power Systems*, vol. 11, no. 3, pp. 1180-1190, Aug. 1996.

[10] S. Suryanarayanan and G. T. Heydt, "Modification to contribution factor formula for unscheduled flows," *IEEE Transactions on Power Systems*, vol. 23, no. 2, pp. 809-810, May 2008.

[11] S. Cvijic and M. D. Ilic. "Part I: A new framework for modeling and tracing of bilateral transactions and the corresponding loop flows in multicontrol area power networks," *IEEE Transactions on Power Systems*, 29(6):2706–2714, Nov. 2014.

[12] C. Zhang, J. Wu, Y. Zhou, M. Cheng, C. Long, "Peer-to-Peer energy trading in a Microgrid," *Applied Energy*, vol. 220, pp. 1-12, June 2018.

[13] D. K. Molzahn et al., "A Survey of Distributed Optimization and Control Algorithms for Electric Power Systems," *IEEE Transaction on Smart Grid*, vol. 8, no. 6, pp. 2941-2962, Nov. 2017.

[14] X. Sun, D. T. Phan and S. Ghosh, "Fully decentralized AC optimal power flow algorithms," *IEEE Power & Energy Society General Meeting*, Vancouver, BC, pp. 1-5, July 2013.

[15] T. Erseghe, "Distributed optimal power flow using ADMM," *IEEE Transactions on Power Systems*, vol. 29, no. 5, pp. 2370-2380, Sept. 2014.

[16] H. Kim and R. Baldick, "Coarse-grained distributed optimal power flow," *IEEE Transaction on Power Systems,* vol. 12, no. 2, pp. 932-939, May 1997.

[17] R. Baldick, B. H. Kim, C. Chase and Yufeng Luo, "A fast distributed implementation of optimal power flow," *IEEE Transactions on Power Systems*, vol. 14, no. 3, pp. 858-864, Aug. 1999.

[18] S. Tosserams, L. F. Etman, P. Y. Papalambros, and J. E. Rooda, "An augmented Lagrangian relaxation for analytical target cascading using the alternating directions method of multipliers," *Structural and Multidisciplinary Optim*ization, vol. 31, no. 3, pp. 176–189, Feb. 2006.

[19] A. Kargarian et al., "Toward distributed/decentralized DC optimal power flow implementation in future electric power systems," *IEEE Transaction on Smart Grid*, vol. 9, no. 4, pp. 2574-2594, July 2018.

[20] B. H. Kim and R. Baldick, "A comparison of distributed optimal power flow algorithms," *IEEE Transactions on Power Systems*, vol. 15, no. 2, pp. 599-604, May 2000.

[21] X. Zhu, X. Han, M. Yang, Y. Xu, S. Wang, "Distributed online optimal power flow for distribution system," *International Journal of Electrical Power & Energy Systems*, vol. 120, Mar. 2020.

[22] R. Pinto, R. J. B., J. Sumaili, M. A. Matos, "Distributed multi-period three-phase optimal power flow using temporal neighbors," *Electric Power Systems Research*, vol. 182, May 2020.

[23] E. Dall'Anese, H. Zhu and G. B. Giannakis, "Distributed optimal power flow for smart microgrids," *IEEE Transactions on Smart Grid*, vol. 4, no. 3, pp. 1464-1475, Sept. 2013.

[24] D. K. Molzahn, I. A. Hiskens, "A survey of relaxations and approximations of the power flow equations," *Foundations and Trends in Electric Energy Systems*, vol. 4, no. 1-2, pp. 1-221, Feb. 2019.

[25] S. H. Low, "Convex relaxation of optimal power flow–Part II: Exactness," *IEEE Transactions on Control of Network Systems*, vol. 1, no. 2, pp. 177–189, June 2014.

[26] L. Yang, J. Luo, Y. Xu, Z. Zhang and Z. Dong, "A distributed dual consensus ADMM based on partition for DC-DOPF with carbon emission trading," *IEEE Transactions on Industrial Informatics*, vol. 16, no. 3, pp. 1858-1872, Mar. 2020.

[27] S. Paul, S. Thiébaux. "Distributed multi-period optimal power flow for demand response in microgrids," *ACM Sixth International Conference on Future Energy Systems*, pp. 17-26. July 2015.

[28] B. Stott, J. Jardim and O. Alsac, "DC power flow revisited," *IEEE Transactions on Power Systems*, vol. 24, no. 3, pp. 1290-1300, Aug. 2009.

[29] G. Cohen, "Auxiliary problem principle and decomposition of optimization problems," *Journal of Optimization Theory and Application*, vol. 32, no. 3, pp. 277-305, Nov. 1980.

[30] D. Hur, J. K. Park, and B. H. Kim, "Evaluation of convergence rate in the auxiliary problem principle for distributed optimal power flow," *IEEE Proceedings Generation, Transmission and Distribution*, vol. 149, no. 5, pp. 525–532, Sep. 2002.

[31] W. Bukhsh, A. Grothey, K. McKinnon, and P. Trodden, "Local solutions of the optimal power flow problem," *IEEE Transactions on Power Systems*, vol. 28, no. 4, pp. 4780-4788, Nov. 2013.

[32] C. Grigg et al., "The IEEE Reliability Test System-1996. A report prepared by the Reliability Test System Task Force of the Application of Probability Methods Subcommittee," *IEEE Transactions on Power Systems*, vol. 14, no. 3, pp. 1010-1020, Aug. 1999.

[33] Open Access Same Time Information System (OASIS) of California electricity market. <http://oasis.caiso.com/>.

[34] System Advisor Model Version 2017.9.5 (SAM 2017.9.5). National Renewable Energy Laboratory. Golden, CO.